An Adaptive Weighted Wi-Fi FTM-Based Positioning Method in an NLOS Environment

Minghao Si, Yunjia Wang, Chee Kiat Seow, Hongji Cao, Hui Liu, and Lu Huang

***Abstract*—In the field of indoor positioning, Wi-Fi FTM is a new technology for realizing high-precision positioning. However, errors caused by clock drift and non-line-of-sight (NLOS) signals affect its positioning accuracy. When receiving NLOS signals, most existing positioning algorithms only delete these signals, which decreases the number of nodes and may decrease accuracy. To address this issue, this paper proposed an adapted weighted positioning method under the NLOS environment. First, this method includes a compensation model to decrease the error caused by clock drift and multipath. Additionally, it can evaluate ranging results and improving the positioning accuracy by assigning greater weight to better ranging results. To verify the effectiveness and feasibility of the proposed method, a positioning experiment is performed under an NLOS environment. The results show that our proposed method is suitable for positioning in a completely NLOS environment and effectively improves the positioning accuracy. Compared with the traditional least squares-based method and the inverse distance weighting-based positioning method, the mean error of the proposed method outperformed by approximately 30% and 20% respectively.**

***Index Terms*—Indoor Positioning, Wi-Fi Fine Time Measurement, Ranging Compensation, Naive Bayes Classification**

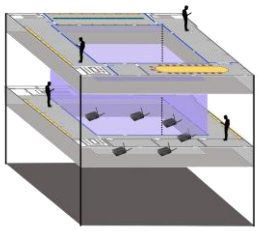

- **A new positioning technology is developed based on Wi-Fi FTM;**
- **Positioning is performed under an NLOS environment, where people and Wi-Fi are separated by glass;**
- **Two models are built to improve the ranging accuracy and positioning accuracy**

I. Introduction

PROVIDING accurate real-time positioning results has always been a challenge for location-based services (LBS). In an outdoor environment, the Global Navigation Satellite System (GNSS) could provide positioning with metre-level accuracy, whereas in an indoor environment, many technologies have been used to implement universal metre-level positioning, such as ultrawide-band (UWB)[1], Bluetooth, Wireless Fidelity (Wi-Fi)[2-4], Radio Frequency Identification (RFID), Computer Vision, ultrasonic, inertial navigation system (INS) [5], pseudolite[6], geomagnetic field, visible light, etc.[7]. Among these technologies, Wi-Fi has always been a research hotspot, and considerable work has been performed due to its wide employment and easy implementation.

The Wi-Fi-based positioning method is mainly implemented by fingerprints using received signal strength indication (RSSI) or channel state information (CSI)[8]. However, these methods need to build offline fingerprint libraries, which consume considerable manpower and time. In 2016, IEEE 802.11 mc standardized the Fine Time Measurement (FTM) protocol, which can provide metre-level positioning accuracy by measuring the round-trip time (RTT) of the Wi-Fi signal between the user and Wi-Fi equipment [9]. The hardware and development platforms that support the protocol were officially available in September 2018. At present, this technology can only be implemented on Google Pixel smartphones with Android version 9.0 and above. Compared with methods based on RSSI, this new technology does not need training offline, which saves considerable labour.

However, the methods based on the new technology may perform worse in some complex environments where the direct path between the transceivers is blocked and only Non-Line-Of-Sight (NLOS) transmission exists or where the distance between transceivers is too long [10-12]. In the first case, the ranging error is due to its ranging mechanism (IEEE Std 802.11, 2016). Methods based on Wi-Fi FTM is affected by NLOS transmission, and so do most wireless signal-based indoor positioning methods [12-14]. Much work has been done to solve the problem, although most associated research only performs Line-Of-Sight (LOS) or NLOS identification and then eliminates the NLOS signals during positioning phase. These methods are not suitable when positioning in a completely NLOS environment because after eliminating the NLOS signals, the number of signals available for positioning is less than the minimum number of signals required for 2D positioning [11,15]. In the second case, the ranging error is due to clock drift. As the

"This work was supported in part by the National Key Research and Development Program of China under Grant 2016YFB0502102."

Minghao Si, Yunjia Wang, Hongji Cao are with the China University of Ming and Technology and Key Laboratory of Land Environment and Disaster Monitoring, Xuzhou 221116, China, (e-mail: hmsi@cumt.edu.cn; wyjc411@163.com; hjcao@cumt.edu.cn; lh199002160015@126.com)

Chee Kiat Seow is with the School of Computing Science, University of Glasgow, Sir Alwyn Williams Building, Glasgow G12 8RZ, Scotland, United Kingdom. (e-mail: CheeKiat.Seow@glasgow.ac.uk)

Lu Huang is with the 54th Research Institute of China Electronics Technology Group Corporation, Shijiazhuang 050081, China (e-mail: hlcetc54@163.com).

ranging results are computed by double-sided two-way ranging (DS-TWR) using timestamps, the ranging results include an error proportional to the actual distance.

In conclusion, it is of great importance to solve the problem of positioning in a complex NLOS environment and to decrease the error caused by NLOS and clock drift. Thus, the key objective of this paper is to propose an adapted weighted Wi-Fi FTM-based positioning method in the NLOS environment. The contributions of this article are summarized as follows.

1) To decrease the ranging error caused by clock drift and multipath, a compensating model is built. According to the DS-TWR analysis, the polynomial is selected to fit the relationship between the ranging error and distance.

2) To decrease the positioning error due to NLOS signals, this article trained an evaluating model based on the Naive Bayes classifier. Additionally, multiple features were extracted from collected Wi-Fi FTM signals to build the model. This process is different from traditional methods that perform an LOS-or-NLOS determination of the signal. The model can help to evaluate each ranging signal before positioning.

3) To fully exploit all ranging signals, an adaptive weighting Wi-Fi FTM-based positioning method is proposed. Compared with traditional methods that use only the LOS signal for calculation, the proposed method uses all the ranging results in positioning based on weighted least squares to improve positioning accuracy.

This article is organized as follows. In Section 1, the new indoor positioning technology Wi-Fi FTM is proposed and the need for the investigation and the main purpose of the proposed method are discussed. In Section 2, the main factors affecting the positioning accuracy of Wi-Fi FTM are analysed and some existing work to solve the problem is introduced. In Section 3, the proposed adaptive weighted Wi-Fi FTM-based positioning method is proposed. In Section 4, experiments are presented to validate the advantages of the proposed method with respect to positioning under the NLOS environment. In Section 5, the conclusions are drawn.

II. Related Work

A. Error caused by clock drift

Wi-Fi FTM ranging is based on DS-TWR, whose ranging results include errors caused by clock drift[4]. In this section, the ranging process is introduced, and the error caused by clock drift is analysed.

The ranging process is shown in Fig. 1. Initialization is necessary before ranging to realize the continuous connection between the initiator and the responder. After initialization, FTM frameworks start to be exchanged between the initiator and the responder. First, an FTM request is sent from the responder to the initiator, and after the initiator receives the request, an ACK signal is sent from the initiator to the responder. Subsequently, several FTM frameworks are exchanged.

In Fig. 1, n indicates one FTM structure exchange during the whole FTM procedure, t_{1_n} is the timestamp when the FTM structure is first sent by the responder, t_{2_n} is the timestamp when the FTM structure is received by the initiator, t_{3_n} is the timestamp when the initiator returns the FTM structure to the responder, and t_{4_n} is the timestamp when the FTM structure is finally received by the responder. Using the four timestamps, two time-differences of the initiator and responder can be calculated based on equations (1) and (2).

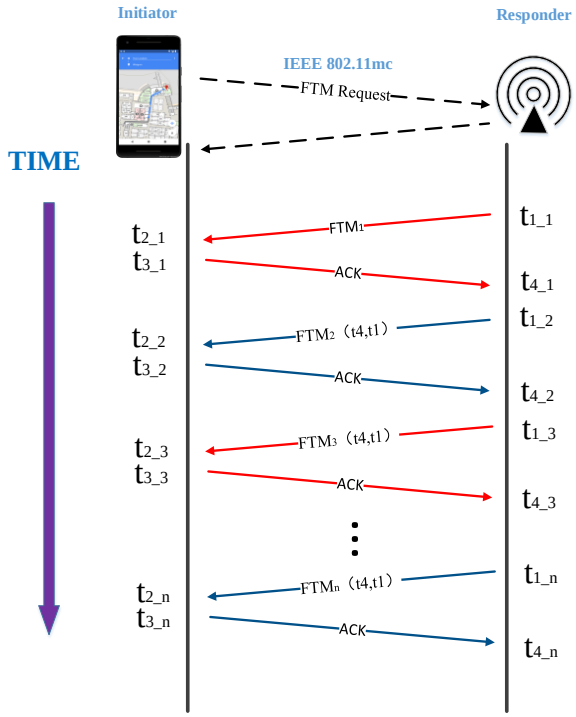

Fig. 1. Production of the Wi-Fi FTM.

$$T_{round} = t_{4\_n} - t_{1\_n} \quad (1)$$

$$T_{reply} = t_{3\_n} - t_{2\_n} \quad (2)$$

A single RTT in one FTM period is calculated by subtracting T_{round} from T_{reply} as shown in equation (3). This calculation is repeated for each FTM structure exchange. As such, the one-way time delay between the initiator and responder, Time of Arrival (TOA) is the average over the number of FTMs per burst, given as .

$$T_{TOA} = \frac{1}{2}(T_{round} - T_{reply}) \quad (3)$$

and ranging distance between the initiator and responder, d, is given as $d = T_{TOA} \times c$ where c is the speed of propagation.

There was minor clock drift between the initiator and the responder. Assuming that the clock drifts of the initiator and the responder are $e_{initiator}$ and $e_{responder}$ respectively, then the flight time is as follows:

$$\hat{T}_{TOA} = \frac{1}{2}\{T_{round}(1 + e_{initiator}) - T_{reply}(1 + e_{responder})\} \quad (4)$$

Therefore, the ranging error caused by clock drift is as follows:

$$e_{clockdrift} = \hat{T}_{TOA} - T_{TOA} \quad (5)$$

$$= \frac{1}{2}\left(T_{round}.e_{initiator} - T_{reply}.e_{responder}\right)$$

$$= \tfrac{1}{2}T_{reply}\left(e_{initiator} - e_{responder}\right) + T_{TOA}.e_{initiator}$$

As T_{reply} is much greater than T_{TOA}, T_{TOA} can be omitted as

shown in equation (6):

$$e_{clockdrift} = \hat{T}_{TOA} - T_{TOA} \approx \frac{1}{2} T_{reply}\left(e_{initiator} - e_{responder}\right) \quad (6)$$

Since T_{reply} and clock drift will grow, $e_{clockdrift}$ will increase.

Researchers have done considerable work to resolve this error. [16] performs a comparison among single-sided two-way ranging (SS-TWR), corrected single-sided two-way ranging (CFO-TWR), symmetric double-sided two-way ranging (SDS-TWR), asymmetric double-sided two-sided two-way ranging (ADS-TWR), and alternative double-sided two-way ranging (AltDS-TWR). All of these have included errors caused by clock drift. [17] calculates the difference between the ranging results and true distance to eliminate the time deviation. However, the performance of the method is affected by the equipment. When the clock drift between nodes is too large, the method performs poorly. [18] proposes an N-ary protocol, which needs to select the desired nodes. In this paper, the Least Squares (LS) method is used to build the error compensation model. Compared with the method in [10], the training data are collected in an LOS environment to improve the performance of the model. Additionally, this method does not require to select the desired nodes.

B. Error caused by NLOS

The TOA estimation of Wi-Fi FTM is based on the propagation time of the signal from the initiator to the responder, and the accuracy of the TOA estimation directly depends on the detection and identification of the direct path (DP) in the received signal. Coppens [19] first proposed the first arrival path method, which works well under a high signal-to-noise ratio. In the case of LOS, the propagation medium of DP is free space and the TOA estimation is more accurate. However, when there are obstacles between the initiator and the responder, the propagation path of DP is NLOS. In the NLOS environment, the DP signal penetrates one or more obstacles, and may undergo multipath delay during propagation. Hence, a positive deviation is introduced in the TOA estimation for LOS model, thereby reducing the accuracy of the TOA estimation, contributing to ranging error. Additionally, due to obstacles such as walls, DP is often not the strongest path in the multipath component at the responder, which further increases the difficulty of DP detection [20].

Regarding the NLOS error, [21] build a Gaussian model to identify NLOS according to the relationship between distance and RSSI. [22] designed a NLOS and LOS identification algorithm based on scenario recognition using Gaussian process regression (GPR). Other methods are shown in [23-26]. However, all of these methods only delete NLOS signals, which makes less use of all ranging results. Additionally, when the number of LOS signals is less than three, the location cannot be calculated, and the accuracy will be decreased. Compared with the above methods, the following proposed method evaluates the ranging results instead of simply eliminating them in order to realize positioning in an NLOS environment.

III. Proposed Method

The proposed adaptive weighted Wi-Fi FTM-based positioning method mainly includes three parts: the error compensation model, the ranging evaluation model, and the weighted least square (WLS) positioning. Before positioning, two models need to be built offline. Firstly, the error compensation model is used to decrease the effect of clock drift and multipath. Ranging errors and ranging results are collected to train the compensation model. Secondly, the ranging evaluation model is built to weigh each ranging result for WLS positioning in the next stage. The model is based on a Naive Bayes classifier to evaluate each ranging result to provide the weighting factor. Finally, the WLS is then applied to achieve the location using the calibrated ranging results and weights from the two models. The whole framework of the proposed method is shown in Fig. 2.

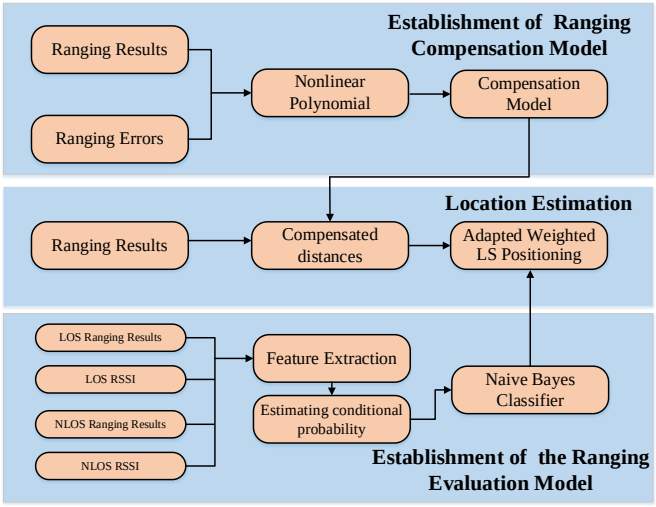

Fig. 2. Flow chart of the proposed method.

A. Error Compensation Model

According to the above analysis, the ranging error caused by clock drift can be assumed to have a nonlinear relationship with the ranging result. However, in the LOS environment, ranging is also affected by other factors, such as multipath and random error [27-29]. To analyse these factors, the ranging results are collected in the LOS environment as shown in Fig. 3. The responder is placed at different distances from the initiator without any obstacle in between.

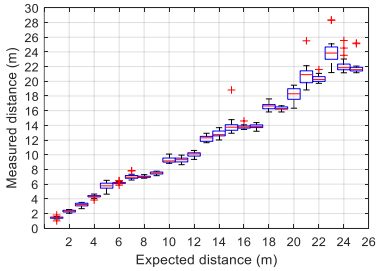

Fig.3. Ranging results at different distances.

It can be found that the ranging error, the number of outlier, and the degree of dispersion will increase as the initiator getting farther away from the responder. This finding is consistent with the experimental results in [30]. In this paper, a nonlinear polynomial model based on least-squares is used to fit the ranging errors and ranging results, as shown in equation (7).

$$e_i = c_0 + c_1\hat{d}_i + c_2\hat{d}_i^2 + \cdots + c_m\hat{d}_i^m \quad (7)$$

where e_i is the ranging error an $\hat{d}_i$ is the ranging distance between the initiator and i^{th} responder. c_m is the m^{th}coefficient for the m ,degree polynomial of $\hat{d}_i$. If there are N number of ranging measurement, then the equation can be expressed as follows:

$$\begin{cases} e_1 = c_0 + c_1\hat{d}_1 + c_2\hat{d}_1^2 + \cdots + c_m\hat{d}_1^m \\ e_2 = c_0 + c_1\hat{d}_2 + c_2\hat{d}_2^2 + \cdots + c_m\hat{d}_2^m \\ \vdots \\ e_N = c_0 + c_1\hat{d}_N + c_2\hat{d}_N^2 + \cdots + c_m\hat{d}_N^m \end{cases} \quad (8)$$

Equation (8) can also be expressed in matrix form:

$$\mathbf{E} = \mathbf{D} \cdot \mathbf{C} \quad (9)$$

$$\mathbf{E} = [e_1 \;\; e_2 \ldots e_N]^T \quad (10)$$

$$\mathbf{D} = \begin{bmatrix} \hat{d}_1^0 & \cdots & \hat{d}_1^m \\ \vdots & \ddots & \vdots \\ \hat{d}_N^0 & \cdots & \hat{d}_N^m \end{bmatrix} \quad (11)$$

$$\mathbf{C} = [c_0 \;\; c_1 \ldots \;\; c_m]^T \quad (12)$$

where $\hat{d}_1^0, \hat{d}_2^0 \cdots \hat{d}_N^0 = 1$

To solve the above equations, the LS solution is used to minimize the sum of square of error residuals of the model according to known data e_i and d_i. The minimum sum of square of residuals is obtained with equation (13), where d is the expected distance and N is the number of ranging results for training. In our experimental campaign, N has 6569 LOS training measurement result collection

$$min(e) = min(\sum_{i=1}^{N}(\hat{d}_i - f(\hat{d}_i, c))^2) \quad (13)$$

Where is e is the total error in range estimation. If (8) meets the condition $N > (m + 1)$, then the coefficients can be calculated using the least square method:

$$\mathbf{C} = (\mathbf{D^T D})^{-1}\mathbf{D^T E} \quad (14)$$

With the obtained coefficients, the ranging error caused by clock drift and multipath can be compensated and the estimated distance can be calculated as shown in equation (15):

$$d_i = \hat{d}_i - e_i \quad (15)$$
$$= \hat{d}_i - (c_0 + c_1\hat{d}_i + c_2\hat{d}_i^2 + \cdots + c_m\hat{d}_i^m)$$

B. Ranging Evaluation Model

To improve the positioning accuracy based on the WLS, each ranging measurement result should be weighted appropriately. In this part, a ranging evaluation model is built to weigh the ranging results based on the Naive Bayes classifier. The procedure of establishing the model is shown in Fig. 4.

Firstly, RSSIs and ranging results should be collected in LOS and NLOS environments, respectively. Secondly, features need to be extracted from collected data. Then, the extracted features need to be analysed for their respective distributions. Finally, with the distributions of features in LOS and NLOS, the conditional probability of the two environments can be obtained.

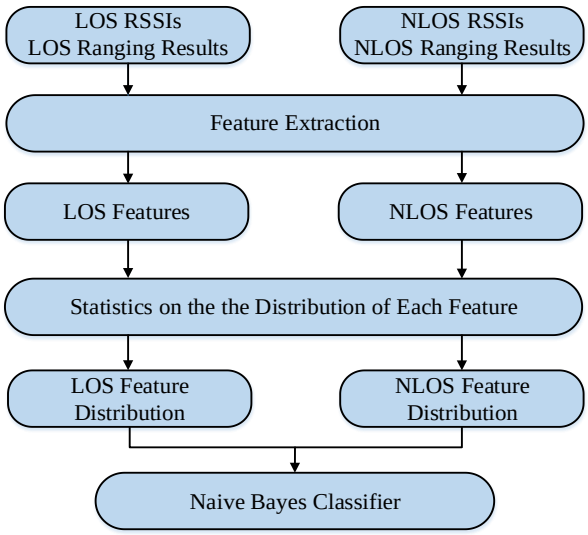

Fig. 4. Flow chart of the naive Bayes classifier.

1) *Feature Extraction*

In this paper, four features are extracted: the ranging measurement ranging result ($\hat{d}_i$), the variance of RSSIs, the collected RSSIs ($\overline{RSSI}_i$) at the initiator and the difference between the theoretical RSSI mapped by measurement ranging results and the collected RSSI. The difference is calculated by subtracting the theoretical RSSI from the collected RSSI as shown in equation (16), and RSSI is the value mapped by the ranging result $\hat{d}_i$ in (17):

$$\text{Feature}_4, \gamma = \left\| \overline{RSSI}_i - RSSI_i \right\| \quad (16)$$

In the same environment, RSSI and distance usually have an exponential relationship [31], and the theoretical RSSI can be calculated by an exponential model as shown in equation (17), where $\mathrm{L}(d_0)$ is the received power when the distance from the responder to the initiator is 1 m; η is the path loss exponent coefficient; and k is a constant.

$$RSSI_i = \mathrm{L}(d_0) + 10 \cdot \eta \cdot \log\left(\frac{\hat{d}_i}{d_0}\right) + k \quad (17)$$

To build the exponential model, the same number of RSSIs is eventually collected at different points. The fitting results are shown in Fig. 5 which demonstrates the close fit between the $\overline{RSSI}_i$ and calculated $RSSI_i$ using $\hat{d}_i$ with γ as the experimental outlier detection. γ is set at 10dB which deems as unreliable $RSSI$ measurement.

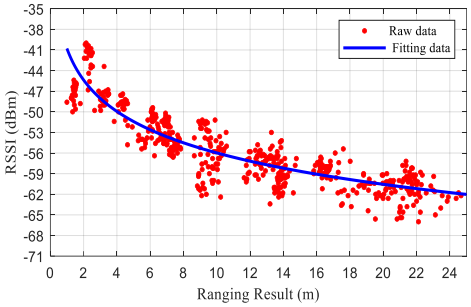

Fig. 5. Fitting result of RSSI

The RSSI variance is computed as shown in equation (18).

$$\sigma_{RSSI}^2 = \frac{\sum_{i=1}^{N}(\widehat{RSSI}_i - \overline{RSSI})^2}{N} \quad (18)$$

2) *Naive Bayes Classifier*

The Naive Bayes classifier is based on the "attribute conditional independence assumption"[32,33] with $\hat{d}_i$ and $\widehat{RSSI}_i$ as independent features. Based on this assumption, the posterior probability of the class can be calculated as (19), where p is the number of RSSI data collection by the initiator with respect to a responder at the i^{th} measurement, $\widehat{RSSI}_i$. In the paper, all the data needs to be divided into two class categories, namely $c = LOS$ or $c = NLOS$.

$$\mathrm{P}\left(\mathrm{c}\middle|\widehat{RSSI}_i\right) = \frac{P(c)P\left(\widehat{RSSI}_i\middle|\mathrm{c}\right)}{P(\widehat{RSSI}_i)} = \frac{P(c)}{P(\widehat{RSSI}_i)}\prod_{k=1}^{p} P(\widehat{RSSI}_{i,k}|c) \quad (19)$$

Because $\mathrm{P}(\widehat{RSSI}_i)$ is the same for both LOS and NLOS, the expression of the naive Bayes classifier can be expressed as follows:

$$\mathrm{P}\left(\mathrm{c}\middle|\widehat{RSSI}_i\right) \equiv \arg\max_{c\in LOs,NLOS} P(c)\prod_{k=1}^{p} P(\widehat{RSSI}_{i,k}||c) \quad (20)$$

The training process of the Naive Bayes classifier requires two steps. First, it needs to estimate the prior probability P(c) of two categories based on the LOS training data set and NLOS training data set. Then, estimate the conditional probability $\mathrm{p}\left(\widehat{RSSI}_i\middle|\mathrm{c}\right)$. According to [21,34,35], the conditional probability is formed as shown in equation (21). Finally, during positioning, the posterior probability, $\mathrm{P}\left(\mathrm{c}\middle|\widehat{RSSI}_i\right)$ is used as the weight of the ranging result, w_i in (23)

$$\mathrm{p}\left(\widehat{RSSI}_{i,k}\middle|\mathrm{c}\right) = \frac{1}{\sqrt{2\pi\sigma_{RSSI}^2}}\exp\left(-\frac{(\widehat{RSSI}_{i,k} - \overline{RSSI})^2}{2\sigma_{RSSI}^2}\right) \quad (21)$$

C. Weighted Least Square

In this paper, a weighted least square (WLS) is used to obtain the 2-D coordinates of the initiator. First, the initial coordinate of the initiator is set as $\mathrm{X} = (X_0, Y_0)$, the coordinates of responders are (X_i, Y_i), and the calibrated ranging results are d_i obtained in (15). Then, we use the least square to approximate the correction matrix Δ as shown in equation (22).

$$\Delta = (\mathbf{A^T W A})^{-1}\mathbf{A^T W E} \quad (22)$$

where $\mathbf{W}$ is the weight matrix, $\boldsymbol{E}$ is the error matrix, and $\mathbf{A}$ is the coefficient matrix as follows

$$\mathbf{W} = \mathrm{diag}(w_i) \quad (23)$$

$$e_i = d_i - \rho_0^i \quad (24)$$

$$A^i = \left[\frac{X_i - X_0}{\rho_0^i}, \frac{Y_i - Y_0}{\rho_0^i}\right] \quad (25)$$

$$\Delta = [dX, dY]^T \quad (26)$$

In the above equations, w_i is the weight of the i^{th} ranging result arises from $\mathrm{P}\left(\mathrm{c}\middle|\widehat{RSSI}_i\right)$ and ρ_0^i is the distance between the initial coordinate of the initiator and the coordinate of the responder in the iteration as $\rho_0^i = \sqrt{(X_0 - X_i)^2 + (Y_0 - Y_i)^2}$. After obtaining Δ, the coordinates of the initiator need to be updated as follows:

$$\mathrm{X} = \mathrm{X} + \Delta = (X_0 + dX, Y_0 + dY) \quad (27)$$

Then, we repeat the above process to constantly update Δ and X until Δ is smaller than a threshold or the number of iterations is larger than a threshold. When the iteration is complete, X is our final coordinate of the initiator. Δ is set as 1×10^{-7} while 3 rounds of iteration are suffice for convergence.

IV. Experiment

A. Analysis of the Error Compensation Model

In this section, the performance of the error compensation model is evaluated. Two data sets were collected, including training data and testing data. The training data is collected in the LOS environment while the testing data is collected in both LOS and NLOS environments as shown in Fig. 6.

Fig. 6 Collecting training data and testing data

In this experiment, 6569 samples were collected as training data using $\gamma = 10dB$ as the guideline to remove noisy and unreliable measurement especially at long distances for distance up to 25m as shown in Fig 7. 6500 samples are collected as testing data which consists of 3250 LOS samples and 3250 NLOS samples. Each sample contains two elements: $\widehat{RSSI}_i$ and ranging result, $\hat{d}_i$. The training data were used to fit the error compensation model. As mentioned in section III, a nonlinear polynomial model was built to calibrate the ranging result, and the coefficients are [-1.317, -1.001, 0.4241, 0.1763] with η calculated as 1.38, as shown in equation (28) and the fitting result is shown in Fig. 7.

$$d_i = \hat{d}_i - e_i = \hat{d}_i - (-1.317 - 1.001\hat{d}_i + 0.424\hat{d}_i^2 + 0.176\hat{d}_i^3) \quad (28)$$

This article has been accepted for publication in a future issue of this journal, but has not been fully edited. Content may change prior to final publication. Citation information: DOI 10.1109/JSEN.2021.3124275, IEEE Sensors Journal

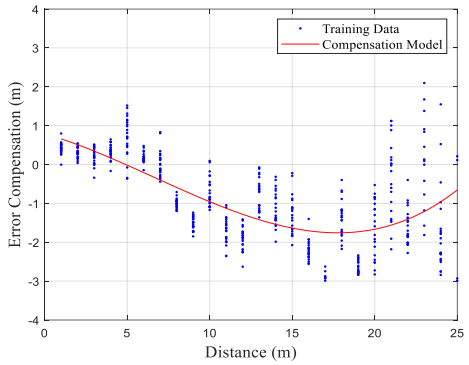

Fig. 7. Fitting result of the compensation model

To test the robustness of the model, the testing data were used to evaluate the performance of the model. Table 1 illustrates the accuracy of the compensated and uncompensated testing data in LOS environment where their mean ranging errors are 1.31 m and 1.82 m respectively. The performance gain is approximately 28%. Table II shows that the mean ranging errors of the compensated and uncompensated model in the NLOS environment are 3.72 m and 4.17 m respectively, achieving a performance gain of 10%. The compensation model can compensate both measured value in both LOS and NLOS environments although the gain in NLOS environment is less as the training data used is in LOS environment. In general, according to [36], e_i in (28) can be further split into three error components, namely $e_{clockdrift}$, e_{nlos} and e_{random} where $e_{clockdrift}$ is error caused by clock drift as shown in (6) . e_{nlos} is the error caused by NLOS propagation while e_{random} is the Gaussian measurement noise. As such, in (28), $d_i = \hat{d}_i - e_i \rightarrow \hat{d}_i - (e_{clockdrift} + e_{nlos} + e_{random})$. As such, the compensation model intent is mainly to provide least square correction factor to minimize $e_{clockdrift}$ and e_{random} with training data obtained in LOS environment, the performance gain is naturally greater in LOS environment than in NLOS environment as shown in Table I and II respectively. The reduction of NLOS error will need to leverage on our proposed ranging evaluation model that pivots on weighted least square using the LOS/NLOS weight arise from NB classifier forming our proposed Wi-Fi FTM- based Positioning algorithm as shown in next section.

Fig. 8 illustrates the cumulative distribution function (CDF) of the ranging errors. As shown, ranging error of less than 2m is achieved for 62% and 85% of time for uncompensated and compensated model respectively, demonstrating an improvement of 25%. The ranging errors that are lower than 1 m are associated with the larger errors in the collected data set at a distance greater than 20 metres, which impacts the effect of the fitting even though some had been identified by feature parameter γ.

TABLE I
LOS RANGING ERROR COMPARISON/(M)

Error	Min (m)	Max (m)	Mean (m)
Compensated	0.35	4.16	1.31
Uncompensated	0.47	4.96	1.82

TABLE II
NLOS RANGING ERROR COMPARISON/(M)

Error	Min (m)	Max (m)	Mean (m)
Compensated	0.39	16.83	3.72
Uncompensated	0.51	17.38	4.17

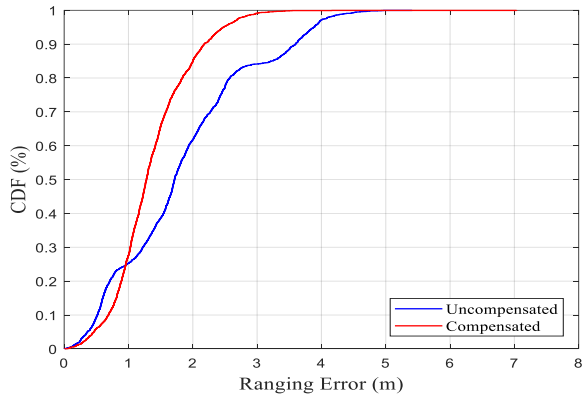

Fig. 8. Cumulative distribution of ranging errors.

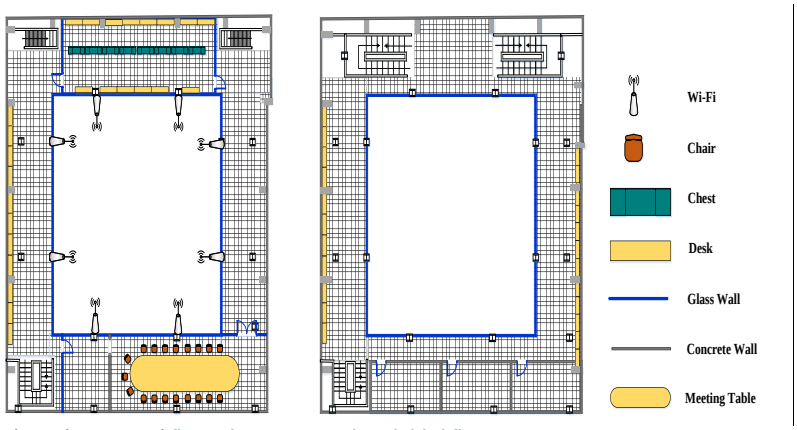

a) Environmental floor plan at second and third floor

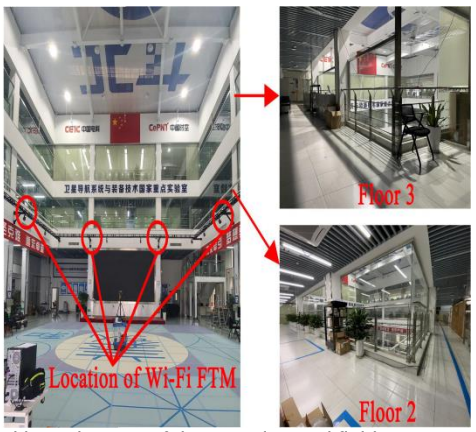

b) Real scene of the experimental field

Fig. 9. Experiment environment

B. Adapted Weighted Wi-Fi FTM-Based Positioning Experiment

In this section, the performance of the proposed adaptive weighting Wi-Fi FTM positioning (AW-WFP) algorithm based on ranging calibration and signal evaluation is evaluated. The experimental campaign is conducted in a typical indoor environment at two floor levels as shown in Fig. 9. As shown in Fig 9(a), eight Wi-Fi FTM Access points (APs) are installed on the wall at first floor and at around 0.63 m below the floor of the second floor contributing NLOS measurement at both indoor location at second and third level. There are various objects in these two indoor environments such as desk and tables as depicted in the legend of the figures. The conditional probability $P(\widehat{RSSI}_i|\mathrm{c})$ in (21) was trained using Gauss regression model in [20] with the training data to obtain the LOS conditional probability $P(\widehat{RSSI}_{i,}|\mathrm{c}=\mathrm{LOS})$. If the ranging measurement result is more than $\pm\sigma_{RSSI,LOS}$ from the $\widehat{RSSI}$ using (18), it will be treated as NLOS ranging result, hence $P(\widehat{RSSI}_{i,}|\mathrm{c}=\mathrm{NLOS})$. It should be noted that all the APs are separated from the testing point by glass walls and all the ranging results can be seen as NLOS as shown in Fig 9(b). For the experimental campaign, a Google Pixel 3 was used to collect data at 146 locations covering the two floors at level 2 and level 3. Each of the 146 locations was evaluated for 30 s before transit to next location test point and its positioning result update frequency was 1 Hz. Since there will 5 samples/sec of RSSI collection, there will 150 samples of RSSI measurement at each location to contribute to the conditional probability $P(\widehat{RSSI}_{i,k}|\mathrm{c})$ and hence posterior probability $\mathrm{P}(\mathrm{c}|\widehat{RSSI}_i)$ in (20). All collected data were processed by MATLAB 2019a software.

The proposed method was compared with the traditional Wi-Fi FTM positioning (T-WFP) method using the least square algorithm and inverse distance weighting Wi-Fi FTM positioning (IDW-WFP) based on the weighted least square algorithm introduced in [37]. In the experimental campaign, all ranging results used by the three methods are calibrated using (28) for fair comparison. The positioning errors and mean errors of three methods at each location test point are shown in Table III and Fig. 10. As shown in Fig. 10, the AW-WFP method has less positioning errors than other two methods. In Table III, the mean positioning accuracy, and the root-mean-square error (RMSE) of the AW-WFP are 2.931 m and 4.203 m, respectively. Compared with the IDW-WFP and T-WFP, our proposed AW-WFP method has its mean error decreased by 0.747 m and 1.204 m respectively showing a performance improvement of 20.3% and 29.1% respectively. Similarly, RMSE is decreased by 0.993 m and 1.669 m respectively with an improvement of 19.1% and 28.4 % respectively. Moreover, 80% of the location test points of the AW-WFP have a positioning error below 3.822 m and outperforms IDW-WFP and T-WFP by 23.2% and 32.3% respectively. It should be noted that we are conduct positioning in a fully NLOS environment as all ranging measurement results are NLOS. As such, the positioning accuracy is worse than that of other localization methodology in the literature that performed positioning in a normal environment [10,17,21,30]. This demonstrates the robustness of our proposed AW-WFP methodology.

TABLE III
POSITIONING ERROR COMPARISONS/(M).

Error	Min	Max	Mean	RMSE	80% Error
AW-WFP	0.004	19.281	2.937	4.203	3.822
IDW-WFP	0.022	21.262	3.684	5.196	4.977
T-WFP	0.093	25.069	4.141	5.873	5.649

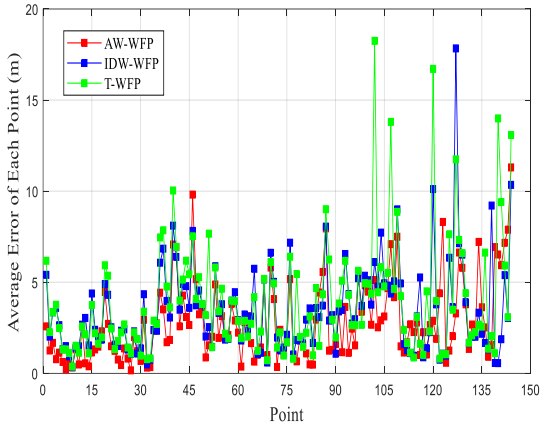

Fig. 10. Point positioning error curves

In addition, an error bar is plotted in Fig. 11 to analyse the stability of positioning algorithms, The blue bar represents the mean error, and the red line segment represents the variance. The red line segment of AW-WFP is the shortest showing the smallest variance among all, indicating that the positioning stability of AW-WFP is the highest.

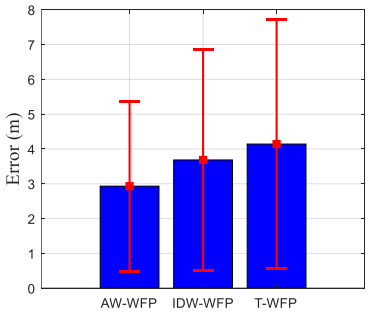

Fig. 11. Error bar of the three positioning methods

Fig. 12 illustrates the performance in cumulative distribution function (CDF) of positioning errors of the three methods. As shown, our proposed AW-WFP method has achieved error less than 2 m for 45.21% of the time as compared to 32.9% and 28.8% by IDW-WFP and T-WFP respectively. Similarly, the proposed AW-WFP achieves error less than 3 m for 65.75% of the time as compared to 48.6% and 49.3% by IDW-WFP and T-WFP respectively. As such, the proposed AW-WFP has demonstrated higher accuracy than the other methods, showing the effectiveness of applying ranging error compensation followed by ranging evaluation model with NB and WLS.

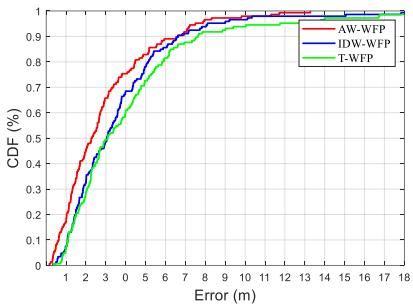

Fig. 12. Cumulative distribution of the three positioning methods

V. Conclusion

In this paper, we focus on positioning in the NLOS environment and propose an adaptive weighted Wi-Fi FTM-based (AW- WFP) positioning method. Firstly, a ranging error compensation model was proposed to decrease the effect of clock drift errors. The error of the calibrated ranging data result is reduced by 28% as compared with the uncalibrated ranging result data using the proposed error compensation model. A ranging evaluation model is then constructed based on the Naive Bayes classifier to provide the LOS/NLOS weighting factor for the calibrated ranging result for the weighted least square localization. The experimental results showed that our proposed method had outperformed the IDW-WFP and T-WFP by 20.1% and 29.1% respectively in terms of mean position error. A performance of 23.2% and 32.3% respectively for RMSE have been observed.

References

[1]Yang, X.F.; Wang, J.; Song, D.P.; Feng, B.Z.; Ye, H. A novel nlos error compensation method based imu for uwb indoor positioning system. Ieee Sensors Journal 2021, 21, 11203-11212.

[2] H. Chen, Y. Zhang, W. Li, X. Tao, and P. Zhang, "ConFi: Convolutional Neural Networks Based Indoor Wi-Fi Localization Using Channel State Information," Ieee Access, vol. 5, pp. 18066-18074, 2017, 2017.

[3] B. Ezhumalai, M. Song, and K. Park, "An Efficient Indoor Positioning Method Based on Wi-Fi RSS Fingerprint and Classification Algorithm," Sensors (Basel, Switzerland), vol. 21, no. 10, 2021 May, 2021.

[4] Y. Yu, R. Chen, L. Chen, S. Xu, W. Li, Y. Wu, and H. Zhou, "Precise 3-D Indoor Localization Based on Wi-Fi FTM and Built-In Sensors," IEEE Internet Of Things Journal, vol. 7, no. 12, pp. 11753-11765, Dec, 2020.

[5] K. Wen, C.K. Seow and S.Y. Tan, "An Indoor Localization and Tracking System Using Successive Weighted RSS Projection", IEEE Antennas and Wireless Propagation Letters, pp. 1620-1624, Vol. 19, Issue 9, Sep 2020.

[6] X. Li, P. Zhang, J. Guo, J. Wang, and W. Qiu, "A New Method for Single-Epoch Ambiguity Resolution with Indoor Pseudolite Positioning," Sensors, vol. 17, no. 4, Apr, 2017.

[7] A. Basiri, E. S. Lohan, T. Moore, A. Winstanley, P. Peltola, C. Hill, P. Amirian, and P. F. e. Silva, "Indoor location based services challenges, requirements and usability of current solutions," Computer Science Review, vol. 24, pp. 1-12, May, 2017.

[8] H. Liu, H. Darabi, P. Banerjee, and J. Liu, "Survey of wireless indoor positioning techniques and systems," Ieee Transactions on Systems Man And Cybernetics Part C-Applications And Reviews, vol. 37, no. 6, pp. 1067-1080, Nov, 2007.

[9] "IEEE Standard for Information technology--Telecommunications and information exchange between systems Local and metropolitan area network--Specific requirements Part 11: Wireless LAN Medium Access Control (MAC) and Physical Layer (PHY) Specifications Amendment 5: Preassociation Discovery," IEEE Std 802.11aq-2018 (Amendment to IEEE Std 802.11-2016 as amended by IEEE Std 802.11ai-2016, IEEE Std 802.11ah-2016, IEEE Std 802.11aj-2018, and IEEE Std 802.11ak-2018), pp. 1-69, 2018.

[10] M. Sun, Y. J. Wang, S. L. Xu, H. X. Qi, and X. X. Hu, "Indoor Positioning Tightly Coupled Wi-Fi FTM Ranging and PDR Based on the Extended Kalman Filter for Smartphones," Ieee Access, vol. 8, pp. 49671-49684, 2020.

[11] H. Zhang, S.Y. Tan and C.K. Seow, "TOA-based indoor localization and tracking with inaccurate floor plan map via MRMSC-PHD filter", IEEE Sensors journal, pp. 9869-9882, vol. 10, issue 21, Nov 2019.

[12] L. Cheng, Y. Li, M. Xue, and Y. Wang, "An Indoor Localization Algorithm Based on Modified Joint Probabilistic Data Association for Wireless Sensor Network," Ieee Transactions on Industrial Informatics, vol. 17, no. 1, pp. 63-72, Jan, 2021.

[13] B. Cao, S. Wang, S. Ge, and W. Liu, "Improving Positioning Accuracy of UWB in Complicated Underground NLOS Scenario Using Calibration, VBUKF, and WCA," Ieee Transactions on Instrumentation And Measurement, vol. 70, 2021, 2021.

[14] S. Xu, Y. Wu, X. Wang, and F. Wei, "Indoor 3D visible light positioning system based on adaptive parameter particle swarm optimisation," Iet Communications, vol. 14, no. 20, pp. 3707-3714, Dec 15, 2020.

[15] C.K. Seow and S.Y. Tan, " Non-line-of-sight localization in multipath environments", IEEE Transactions on Mobile Computing, pp. 647-660, Vol. 7, Issue 5, May 2008

[16] J. Sidorenko, V. Schatz, N. Scherer-Negenborn, M. Arens, and U. Hugentobler, "Error Corrections for Ultrawideband Ranging," Ieee Transactions on Instrumentation And Measurement, vol. 69, no. 11, pp. 9037-9047, Nov, 2020.

[17] Y. Yu, R. Chen, Z. Liu, G. Guo, F. Ye, and L. Chen, "Wi-Fi Fine Time Measurement: Data Analysis and Processing for Indoor Localisation," Journal Of Navigation, vol. 73, no. 5, pp. 1106-1128, Sep, 2020.

[18] F. Despaux, A. van den Bossche, K. Jaffres-Runser, and T. Val, "N-TWR: An accurate time-of-flight-based N-ary ranging protocol for Ultra-Wide band," Ad Hoc Networks, vol. 79, pp. 1-19, Oct, 2018.

[19] F. Coppens, " First arrival picking on common - offset trace collections for automatic estimation of static corrections," Geophysical Prospecting, vol. 33, no. 8, pp. 1212-1231, 1985.

[20] D. Cassioli, M. Z. Win, F. Vatalaro, and A. F. Molisch, "Low complexity rake receivers in ultra-wideband channels," IEEE Transactions on Wireless Communications, vol. 6, no. 4, pp. 1265-1275, 2007.

[21] M. Si, Y. Wang, S. Xu, M. Sun, and H. Cao, "A Wi-Fi FTM-Based Indoor Positioning Method with LOS/NLOS Identification," Applied Sciences-Basel, vol. 10, no. 3, Feb, 2020.

[22] H. Cao, Y. Wang, J. Bi, S. Xu, M. Si, and H. Qi, "Indoor Positioning Method Using WiFi RTT Based on LOS Identification and Range Calibration," Isprs International Journal Of Geo-Information, vol. 9, no. 11, Nov, 2020.

[23] K. Han, H. Xing, Z. Deng, and Y. Du, "A RSSI/PDR-Based Probabilistic Position Selection Algorithm with NLOS Identification for Indoor Localisation," Isprs International Journal Of Geo-Information, vol. 7, no. 6, Jun, 2018.

[24] H. J. Jo, and S. Kim, "Indoor Smartphone Localization Based on LOS and NLOS Identification," Sensors, vol. 18, no. 11, Nov, 2018.

[25] C. Jiang, S. Chen, Y. Chen, D. Liu, and Y. Bo, "An UWB Channel Impulse Response De-Noising Method for NLOS/LOS Classification Boosting," Ieee Communications Letters, vol. 24, no. 11, pp. 2513-2517, Nov, 2020.

[26] C. Jiang, J. Shen, S. Chen, Y. Chen, D. Liu, and Y. Bo, "UWB NLOS/LOS Classification Using Deep Learning Method," Ieee Communications Letters, vol. 24, no. 10, pp. 2226-2230, Oct, 2020.

[27] C. Ascher, L. Zwirello, T. Zwick, G. Trommer, and Ieee, "Integrity Monitoring for UWB/INS Tightly Coupled Pedestrian Indoor Scenarios," 2011 International Conference on Indoor Positioning And Indoor Navigation, International Conference on Indoor Positioning and Indoor Navigation, 2011.

[28] A. Wang, Y. Song, and Ieee, Improved SDS-TWR ranging technology in UWB positioning, 2018.

[29] Y. Zhao, J. Guo, J. Zou, P. Zhang, D. Zhang, X. Li, G. Huang, and F. Yang, "A Holistic Approach to Guarantee the Reliability of Positioning Based on Carrier Phase for Indoor Pseudolite," Applied Sciences-Basel, vol. 10, no. 4, Feb, 2020.

[30] L. Banin, U. Schatzberg, and Y. Amizur, "WiFi FTM and map information fusion for accurate positioning."

[31] Y. Shi, Y. Hao, D. Liu, and B. Wang, "Position Estimation Based on RSS and DOA Path Loss Model," Communications, Signal Processing, And Systems, Lecture Notes in Electrical Engineering Q. Liang, J. Mu, M. Jia, W. Wang, X. Feng and B. Zhang, eds., pp. 2582-2592, 2019.

[32] D. Farahiyah, R. M. Romadhoni, S. W. Pratomo, and Acm, Naive Bayes Classifier for Indoor Positioning using Bluetooth Low Energy, 2018.

[33] C. Song, J. Wang, and G. Yuan, "Hidden Naive Bayes Indoor Fingerprinting Localization Based on Best-Discriminating AP Selection," Isprs International Journal Of Geo-Information, vol. 5, no. 10, Oct, 2016.

[34] B. Xu, X. Zhu, and H. Zhu, "RSSI-Fading-Based Localization Approach in BLE5.0 Indoor Environments," Wireless And Satellite Systems, Pt Ii, Lecture Notes of the Institute for Computer Sciences Social Informatics and Telecommunications Engineering M. Jia, Q. Guo and W. Meng, eds., pp. 131-144, 2019.

[35] K. Zhang, Y. Zhang, and S. Wan, Research of RSSI Indoor Ranging Algorithm Based on Gaussian - Kalman Linear Filtering, 2016.

[36] Yu Y, Chen R, Chen L, et al. A Robust Dead Reckoning Algorithm Based on Wi-Fi FTM and Multiple Sensors[J]. Remote Sensing, 2019, 11(5): 504.

[37] J. Talvitie, M. Renfors, and E. S. Lohan, "Distance-Based Interpolation and Extrapolation Methods for RSS-Based Localization With Indoor Wireless Signals," Ieee Transactions on Vehicular Technology, vol. 64, no. 4, pp. 1340-1353, Apr, 2015.

Minghao Si was born in Taicang, Jiangsu Province, China in 1995. He received the B.S. degree in civil engineering from Jinling Institute of Technology, Nanjing, China in 2017. He is currently pursuing the Ph.D degree in the geodesy and survey engineering at CUMT. From 2017 to 2019, He studied geodesy and survey engineering at CUMT. He is currently pursuing the Ph.D degree at CUMT. His research

interests include indoor positioning and navigation, machine learning

Yunjia Wang received the M.S. degree in mine surveying and the Ph.D. degree in mining engineering from CUMT (China University of Mining and Technology), Xuzhou, China in 1988 and 2000, respectively. From 2007 to 2016, He is the president of School of Environment Science and spatial Informatics, CUMT, China. His current research interests include indoor and outdoor seamless positioning, In-SAR, assessment and management of resources and environment and geographic information engineering.

Chee Kiat Seow (M' 02–SM' 13) received the Ph.D. degree from Nanyang Technological University, in 2009. From 2011 to 2018, he was a senior Research Fellow and then a senior lecturer with the School of Electrical and Electronics Engineering, Nanyang Technological University, Singapore. He is currently an assistant professor at University of Glasgow, School of Computing Science, UK since 2019. His research interests include localization methodology/algorithms, physical cyber security, big data and artificial intelligence/machine learning for various applications such as robotics.

Hongji Cao received the bachelor degree in surveying and mapping engineering from Henan Polytechnic University, Jiaozuo, China in 2016. From 2016 to 2018, he studied the cartography and Geographical information engineering at China University of Mining and Technology (CUMT) in Xuzhou, China. He is currently pursuing the Ph.D degree in the geodesy and survey engineering at CUMT

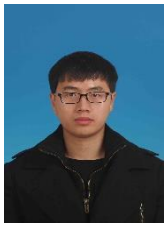

Hui Liu received the B.S. degree in Geographic Information System from China University of Petroleum, Tsingtao, China, in 2011.He is currently working toward the M.S. degree with Surveying and mapping engineering from China University of Mining and Technology, Xuzhou, China. He research interests indoor positioning

LU HUANG was born in Panjin, Liaoning Province, China, in 1991. He received the B.E. in electronic information engineering from Shenyang Ligong University, in 2014 and M.E. degree in Information and Communication Engineering from Harbin Engineering University, in 2017. His research interests include indoor multi-sensor fusion positioning, indoor pseudo-satellite positioning. He participated in five national key R&D projects, published more than 10 academic papers, and applied for three invention patents. He participated in the formulation of several standards in the field of indoor positioning.